Journal of Materials Chemistry A

ARTICLE

# Biomineralization-Inspired Crystallization of Monodisperse α-Mn2O3 Octahedra and Assembly of High-Capacity Lithium-ion Battery Anodes

Received 00th January 20xx,
Accepted 00th January 20xx

DOI: 10.1039/x0xx00000x

www.rsc.org/

Joel Henzie,[*a] Vinodkumar Etacheri,[b] Maryam Jahan,[a] Hongpan Rong,[a] Chulgi Nathan Hong,[b] Vilas G. Pol[*]

## Contents

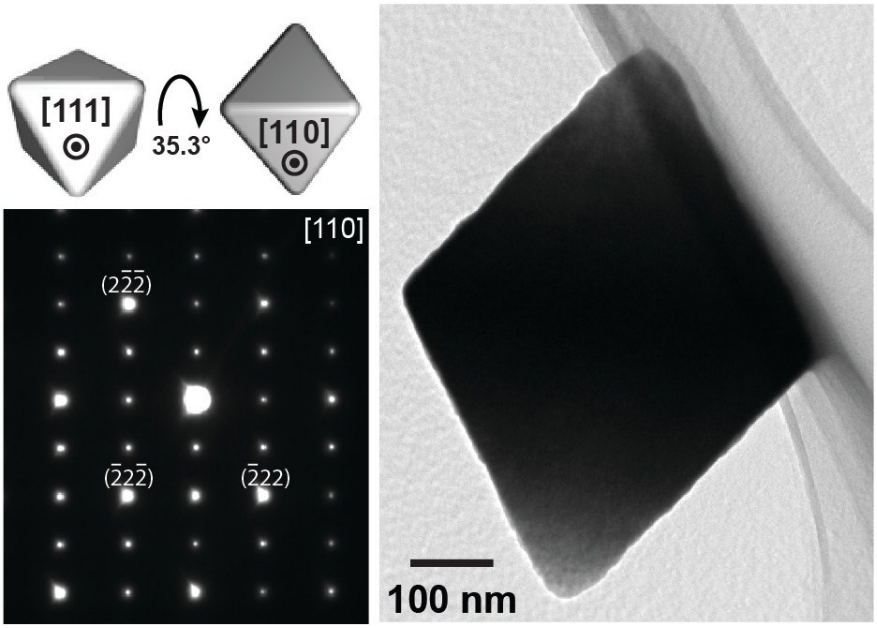


**Figure S1.** The α-$Mn_2O_3$ octahedra were tilted in the TEM to observe the crystal along the [110] direction. The whole particle was imaged by TEM and the collected SAED pattern showed the particle was single crystal and no noticeable unrelated crystallites are present.

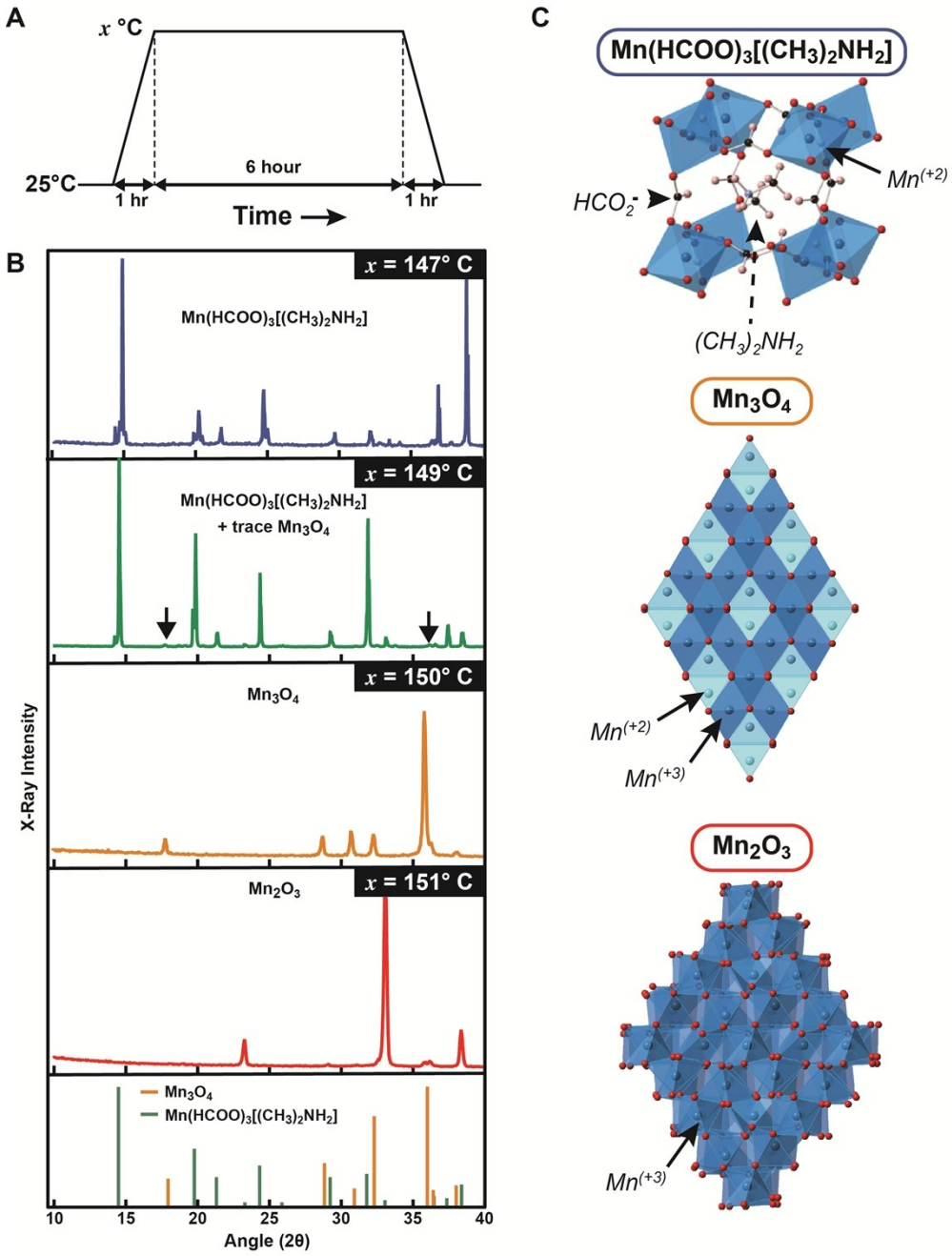


**Figure S2.** Solvothermal experiments conducted at lower temperatures show the phase of the material transforms from $Mn(HCOO)_3[(CH_3)_2NH_2]$ ➔ $Mn_3O_4$ ➔ α-$Mn_2O_3$. All solvothermal experiments were conducted using a 1-hour ramp from room temperature to *x*° *C.*, followed by a 6-hour soak at constant temperature *x*° C, followed by a 1-hour ramp down to room temperature (**A**). Samples generated by this solvothermal method were conducted at different soak temperatures from *x*=147, 149, 150, and 151° C and measured by PXRD (**B**). At *x*=147° C $Mn(HCOO)_3[(CH_3)_2NH_2]$ metal organic frameworks (MOFs) is generated almost exclusively. As temperature is increased to *x*=149° C we can see the emergence of $Mn_3O_4$ (see black arrows), which becomes the primary phase at *x*=150° C. Above *x*=151° C and extending to 180° C we observed α-$Mn_2O_3$ exclusively. The models show the structural relationship between $Mn(HCOO)_3[(CH_3)_2NH_2]$, $Mn_3O_4$, and α-$Mn_2O_3$ (**C**).

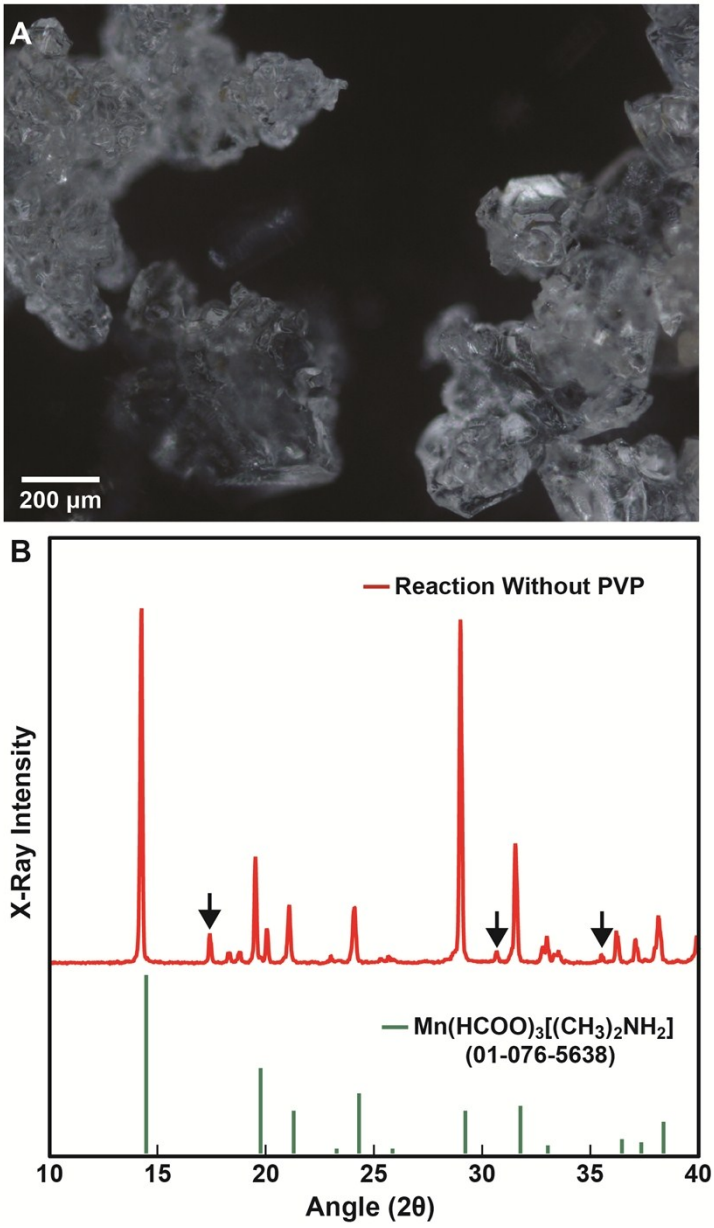


**Figure S3.** Experiments show that PVP was essential to the reaction and omission of PVP yielded $Mn(HCOO)_3[(CH_3)_2NH_2]$ metal organic frameworks (MOFs). The solvothermal reaction was performed without PVP polymer (ie. 4.81 mL of aqueous 50% $Mn(NO_3)_2$ in 35 mL of DMF) at $t$ = 180°C. Omission of PVP yields multiferroic $Mn(HCOO)_3[(CH_3)_2NH_2]$ MOF microcrystals. (**A**) An optical micrograph of the MOF microcrystals. (**B**) PXRD pattern showing the MOF crystals conform closely to the predicted structure for $Mn(HCOO)_3[(CH_3)_2NH_2]$ MOF. The black arrows indicate peaks that correspond to an $Mn_3O_4$ impurity.

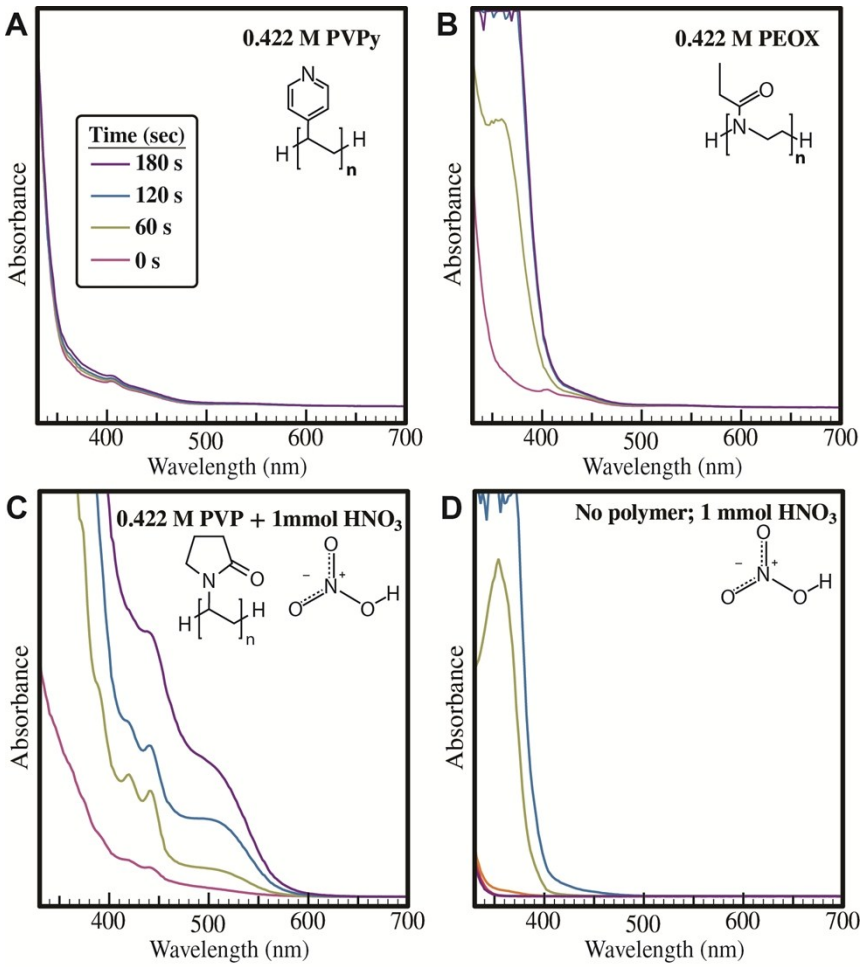


**Figure S4.** Colorimetric measurements show the importance of the pyrrolidone moiety in the standard reaction heated to $t$ = 151°C in an open vial for different times. (**A**) 4.81 mL of aqueous 50% $Mn(NO_3)_2$ was mixed with 0.422 M of poly(4-vinylpyridine) (PVPy; $M_w$~60K) in 35 mL of DMF. (**B**) 4.81 mL of aqueous 50% $Mn(NO_3)_2$ was mixed with 0.422 M of polyethyloxazoline (PEOX; $M_w$~50K) in 35 mL of DMF. (**C**) 4.81 mL of aqueous 50% $Mn(NO_3)_2$ was mixed with 0.422 M of PVP in 35 mL of DMF + 1 millimole of nitric acid ($HNO_3$). (**D**) 4.81 mL of aqueous 50% $Mn(NO_3)_2$ was mixed with 35 mL of DMF + 1 millimole of nitric acid ($HNO_3$). Samples were collected at different times (ie. 0, 60, 120 and 180 seconds) and measured with a UV-Vis spectrophotometer.

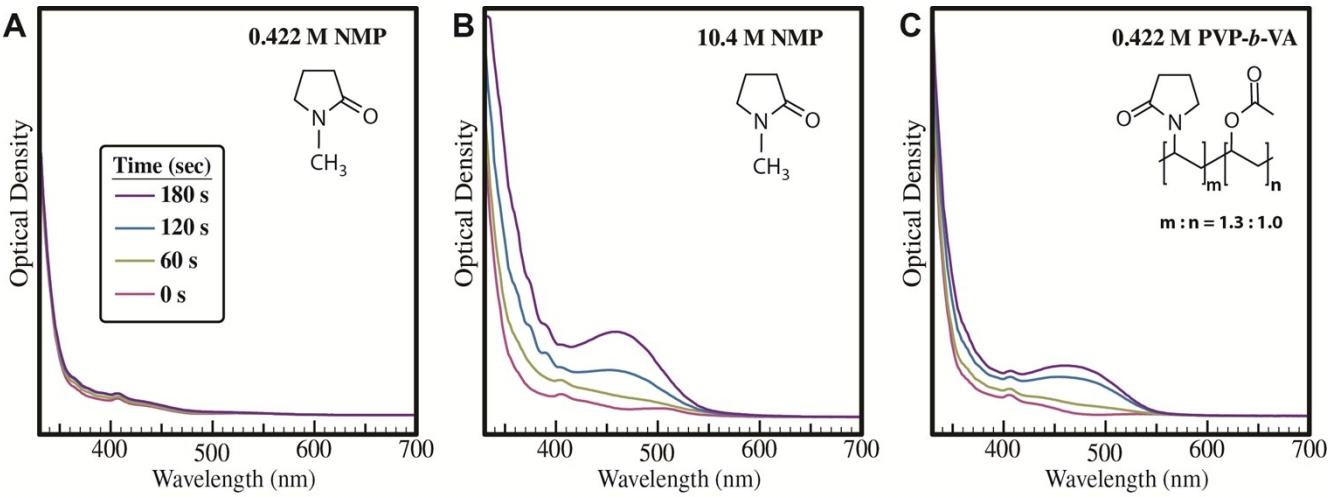


**Figure S5.** Colorimetric measurements show the importance of the PVP microstructure in the standard reaction heated to $t$ = 151°C in an open vial for different times. (**A**) 4.81 mL of aqueous 50% $Mn(NO_3)_2$ was mixed with 0.422 M NMP in 35 mL of DMF. (**B**) 4.81 mL of aqueous 50% $Mn(NO_3)_2$ was mixed with 35 mL of neat NMP (ie. 10.4 M). (**C**) 4.81 mL of aqueous 50% $Mn(NO_3)_2$ was mixed with 0.422 M PVP-*b*-VA in 35 mL of DMF. The figure legend in (**A**) corresponds to all panels. Samples were collected at different times (ie. 0, 60, 120 and 180 seconds) and measured with a UV-Vis spectrophotometer.

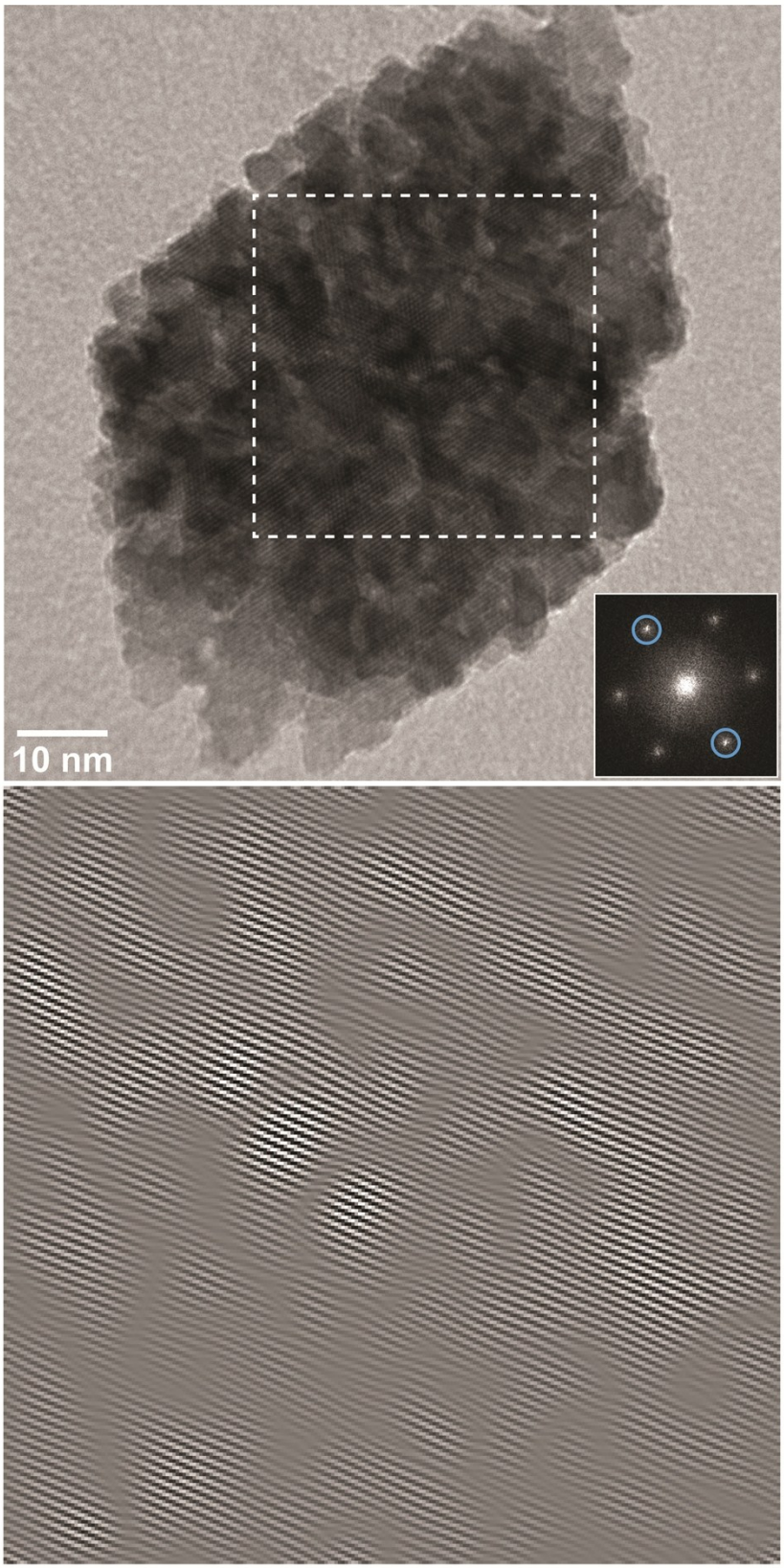


**Figure S6.** The $(101)$ and $(\bar{1}0\bar{1})$ reflections from the Fourier transform of the HRTEM image (Top) were used to construct a moiré image (Bottom). It shows variations in intensity shows that the particle is initially quite porous yet it is still crystalline with a coherent lattice extending across the entire particle and forming a coherent single-crystalline unit.

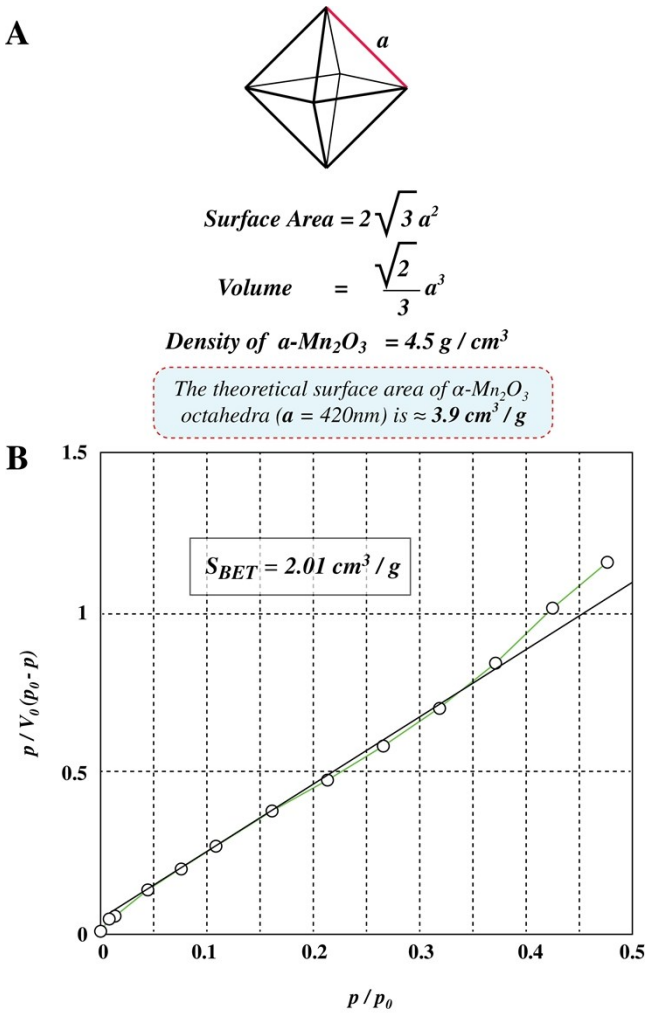


**Figure S7.** An ensemble of α-$Mn_2O_3$ octahedra with edge lengths of $a$ = 420 nm would have a surface area per gram ($cm^3$/gram) of ~3.9 assuming the particle is non-porous and its surface is perfectly flat (**A**). The $N_2$ adsorption isotherm was linear between $0.05<\rho/\rho_0<0.35$ for the as-synthesized α-$Mn_2O_3$ octahedra with an $S_{BET}$ of ~2.01 $cm^3$/gram (**B**).

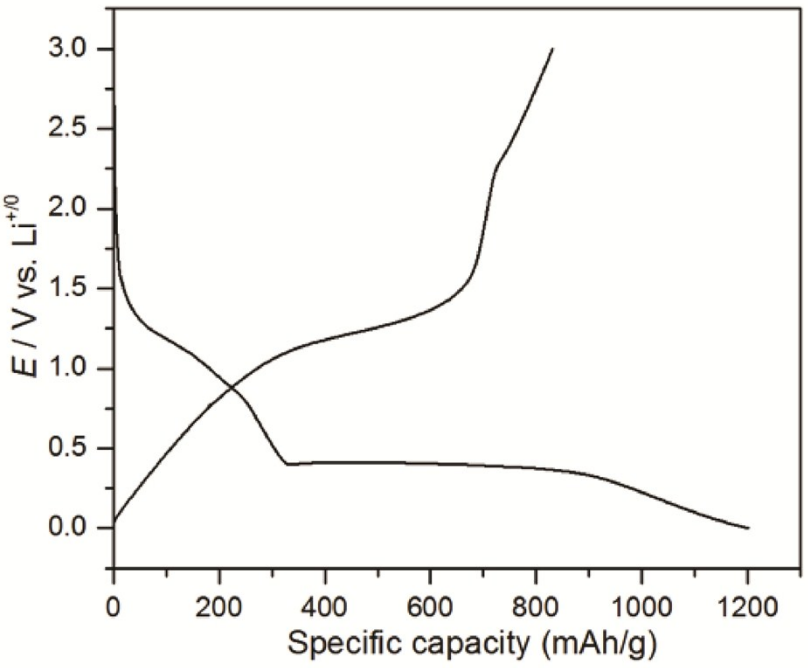


**Figure S8.** First charge-discharge cycle of LIB battery anodes composed of α-$Mn_2O_3$ octahedral nanoparticles.

| Work | Rate performance | Cycling stability | Coulombic efficiency |
|---|---|---|---|
| Octahedral single crystals (This study) | 435 mAh/g at 3.2 A/g current density | 90% after 100 cycles | 99.5 |
| Nanowires (ref 1) | 235 mAh/g at 1 A/g | 100 % after 100 cycles | 98% |
| Hollow spheres (ref 2) | 422 mAh/g at 1.6 A/g | 75% after 100 cycles | 99.7 |
| Hierarchical microspheres (ref 3) | 400 mAh/g at 1.6 A/g | 50% after 50 cycles | Unknown |

**Table S1.** Comparison of rate performance, cycling stability, and Coulombic efficiency of this study to similar work.

**References:**

**1.** Y. Wang, Y. Wang, D. Jia, Z. Peng, Y. Xia and G. Zheng, *Nano Lett.*, 2014, **14**, 1080–1084

**2.** H. Su, Y.-F. Xu, S.-C. Feng, Z.-G. Wu, X.-P. Sun, C.-H. Shen, J.-Q. Wang, J.-T. Li, L. Huang and S.-G. Sun, *ACS Appl. Mater. Interfaces*, 2015, **7**, 8488–8494

**3.** L. Hu, Y. Sun, F. Zhang and Q. Chen, *J. Alloys Compd.*, 2013, **576**, 86–92